

## Article

# The Influence of Branched Chain Length on Different Causticized Starches for the Depression of Serpentine in the Flotation of Pentlandite

Chenxu Zhang <sup>1,2,3</sup>, Yiping Tan <sup>1,2,3</sup>, Fengxiang Yin <sup>1,2,3</sup>, Jiamei Wu <sup>1,2,3</sup>, Lichang Wang <sup>4,\*</sup> and Jian Cao <sup>1,2,3,5,6,\*</sup> <sup>1</sup> School of Minerals Processing and Bioengineering, Central South University, Changsha 410083, China<sup>2</sup> Hunan International Joint Research Center for Efficient and Clean Utilization of Critical Metal Mineral Resources, Central South University, Changsha 410083, China<sup>3</sup> Key Laboratory of Hunan Province for Clean and Efficient Utilization of Strategic Calcium-Containing Mineral Resources, Central South University, Changsha 410083, China<sup>4</sup> School of Geosciences and Info-Physics, Central South University, Changsha 410083, China<sup>5</sup> State Key Laboratory of Mineral Processing, Beijing 100814, China<sup>6</sup> State Key Laboratory of Comprehensive Utilization of Nickel and Cobalt Resources, Jinchang 737100, China

\* Correspondence: wlccsu@csu.edu.cn (L.W.); caojianzu@163.com (J.C.); Tel.: +86-731-88876734 (L.W.); +86-731-88830482 (J.C.)

**Abstract:** Although studies on starch have developed in polymer chemistry research, their structure-activity relationship remains indistinct in the flotation depressants field. In this work, the utilization of five types of causticized starches from different botanical sources as depressants in the flotation of pentlandite/serpentine pure mineral systems was studied. The branched chain length of the starches was quantitatively analyzed using a high-performance anion-exchange chromatography system, and the average branched chain lengths of the causticized starches were obtained. The flotation results demonstrated that the depression effect of all causticized starches on serpentine had a positive correlation with the average branched chain length. Zeta potential tests, FTIR experiments, and XPS analysis confirmed that the causticized starches with a longer branched chain were absorbed more strongly on the serpentine surface. In the present study, the influence of branched chain length on the depression effect of causticized starch was investigated, which deepened our understanding of the depression mechanism of traditional macromolecule depressants and will promote the development of new macromolecule depressants.

**Keywords:** causticized starch; depressant; flotation separation; pentlandite; serpentine

**Citation:** Zhang, C.; Tan, Y.; Yin, F.; Wu, J.; Wang, L.; Cao, J. The Influence of Branched Chain Length on Different Causticized Starches for the Depression of Serpentine in the Flotation of Pentlandite. *Minerals* **2022**, *12*, 1081. <https://doi.org/10.3390/min12091081>

Academic Editor: Saeed Chehreh Chelgani

Received: 4 August 2022

Accepted: 25 August 2022

Published: 26 August 2022

**Publisher's Note:** MDPI stays neutral with regard to jurisdictional claims in published maps and institutional affiliations.



**Copyright:** © 2022 by the authors. Licensee MDPI, Basel, Switzerland. This article is an open access article distributed under the terms and conditions of the Creative Commons Attribution (CC BY) license (<https://creativecommons.org/licenses/by/4.0/>).

## 1. Introduction

Starch is a class of natural, renewable, and biodegradable polysaccharide polymer [1,2]. Most starches are a mixture of unbranched amylose (content < 30%) and branched amylopectin (content >70%) [3,4]. Amylose consists of linear chains linked by (1→4) bonds, while amylopectin consists of linear chains linked by (1→4) bonds and branched chains by (1→6) bonds (Figure 1) [5]. The applications of amylopectin are much broader than those of amylose because of its solubility (linear chains tend to form insoluble semi-crystalline aggregates) [6]. For amylopectin, the branched chains have a clear influence the properties of amylopectin. The main parameter that measures the properties of branched chains is branched chain length, which is defined by the degree of polymerization of the branched chains [7]. For instance, J. Jane revealed that branched chain length has a critical impact on the gelatinization and pasting properties of amylopectin [8]. C. Menzel declared that the branched chain length of amylopectin has significant implications for the thermal and mechanical stability of film materials [9].

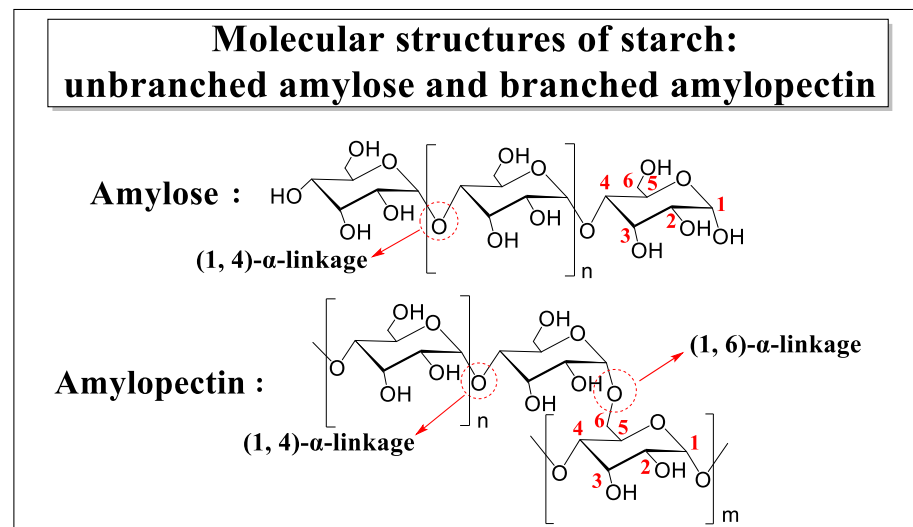


**Figure 1.** Two different molecular structures of starch: unbranched amylose and branched amylopectin.

Starch, starch derivatives, and similar polysaccharides have been frequently used as depressants in the flotation of sulfide and oxide minerals. For example, they can take effect in the depression of millerite [10], galena [11], pyrrhotite [12], pyrite [13], chlorite [14], hematite [15], serpentine [16–20], talc [21–25], forsterite [26], and so forth. At present, the chemical modification of these polymers to improve their depression effect is a research hotspot in mineral processing. D.A. Beattie replaced the hydroxyl groups at positions C2 and C6 of starch with hydroxypropyl groups, which improved the depression effect of the modified product for talc in the flotation of Ni-Cu sulfide ore [21]. F. Tian reported that carboxylated starch showed a superior depression effect towards forsterite in the flotation of ilmenite [26]. In addition, carboxymethyl starch, oxidized starch, and amphoteric starch were shown to facilitate the depression effect of molybdenite [27], graphite [28], and diasporite [29], respectively.

Although starch and modified starch have been frequently used as depressants in mineral processing, there is still a lack of understanding of the relationship between the molecular structure and depression effect. For instance, the influence of branched chain length on the depression effect of starch depressants is still unclear. In order to address this issue, this work investigated the utilization of causticized starches with different branched chain lengths as depressants for serpentine in a pentlandite/serpentine flotation system, which is a common problem in the flotation of Ni-Cu sulfide ore [17,30–32]. This work provided a new approach to study the depression mechanism of starch depressants.

## 2. Materials and Methods

### 2.1. Samples and Reagents

Pure mineral samples of serpentine and pentlandite for micro-flotation tests and other experiments were obtained from Jinchuan, Yingkou in China. The pentlandite sample were crushed, handpicked, and then dry-ground with a porcelain ball mill and dry-sieved to obtain different size fractions. The magnetic separation method was used to remove the pyrrhotite, and the final non-magnetic mineral was the desired product (pentlandite). The samples of pentlandite with particle sizes ranging from  $-74$  to  $+38$   $\mu\text{m}$  were utilized for the micro-flotation tests. The  $-38$   $\mu\text{m}$  size fractions were used for the other tests. The serpentine sample was ground using an agate ball mill and the average particle size of serpentine minerals was about  $4.3$   $\mu\text{m}$ , as measured by a laser particle size analyzer. The X-ray diffraction (XRD) analyses confirmed that the purity of serpentine (lizardite) and pentlandite was very high (Figure 2).

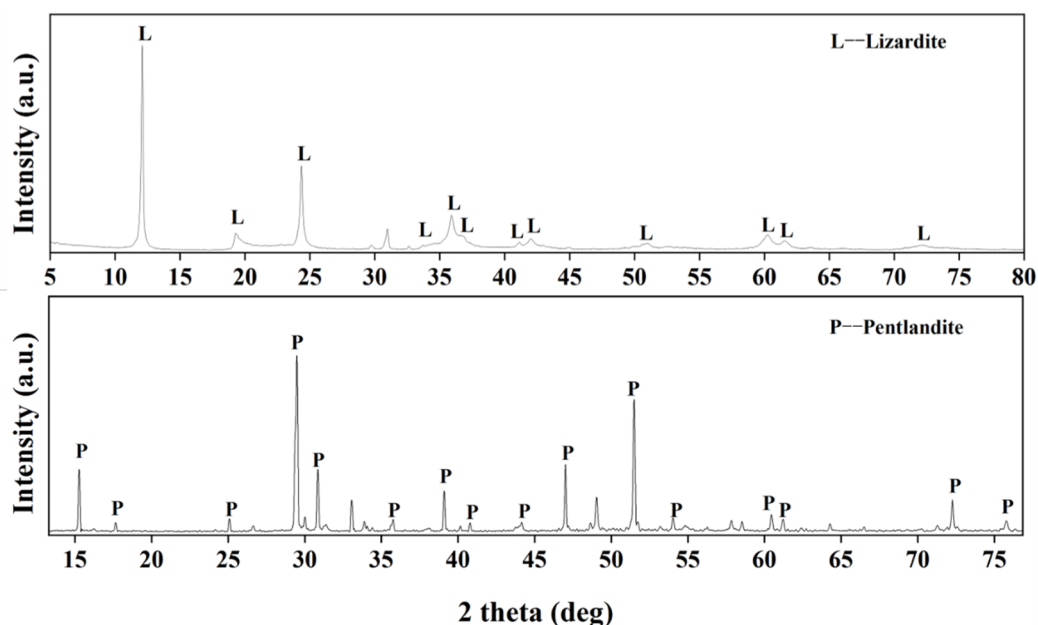


Figure 2. XRD spectra of serpentine (lizardite) and pentlandite samples.

Potassium butyl xanthate (PBX) was used as the sulfide collector [33]. The causticized starches described in Section 2.2 were utilized as depressants for serpentine and methyl isobutyl carbinol (MIBC) acted as the frother [32,34]. Hydrochloric acid (HCl) and sodium hydroxide (NaOH) were used as the pH regulators in micro-flotation and the other tests. Milli-Q water with a resistivity of 18.2 m $\Omega$  cm was utilized in all the experiments. All the reagents described above were of analytical grade.

### 2.2. Causticization of Starch

Due to the poor water solubility of starch, it is generally causticized before use in flotation. Causticized starch was prepared as follows [35,36]: (1) 0.1 g starch and 0.025 g sodium hydroxide were added to 50 mL deionized water in a 100 mL round bottom flask; (2) the mixture was incubated and reacted at 85–90 °C in a sand bath for 40 min; (3) it was then cooled to room temperature to obtain a relatively transparent causticized starch solution.

The difference between original and causticized starch was assessed through scanning electronic microscope images (Figure 3). As can be seen from Figure 3A, the initial starch had a smooth granule surface. However, it can be seen from Figure 3B that the causticized starch had a completely different surface morphology from that of the untreated starch, i.e., the causticized starch had a rough and irregular granule surface.

### 2.3. Determination of Branched Chain Length of Amylopectin

A total of 5 mg oligosaccharide standard of DP4-DP7 (Oligosaccharides Kit, from sigma company) was dissolved in 5 mL of water in a boiling water bath for 60 min; 50  $\mu$ L of sodium acetate (0.6 mol/L), 10  $\mu$ L NaN<sub>3</sub> (2% w/v), and 10  $\mu$ L isoamylase (1400 U) were added and the mixture was incubated at 37 °C for 24 h [37,38]. Thereafter, 0.5% (w/v) sodium borohydride solution was added to the mixture and it was left to stand for 20 h. Then, 600  $\mu$ L of the sample solution was transferred into a centrifuge tube and dried with nitrogen at room temperature. The samples were dissolved in 30  $\mu$ L NaOH (1 mol/L) for 60 min, diluted with 570  $\mu$ L water, and centrifuged at 12,000 r/min for 5 min, to complete the process. Starch samples were treated with the same method as above.

The sample extracts were analyzed by high-performance anion-exchange chromatography (HPAEC) on a CarboPac PA-100 anion-exchange column (4.0 mm  $\times$  250 mm; Dionex) using a pulsed amperometric detector (PAD; Dionex ICS 5000 system) [39,40]. The flow rate

was 0.4 mL/min, the injection volume was 5  $\mu$ L, the solvent system (flow phase) was 0.2 M NaOH or 0.2 M NaOH/0.2 M NaAc, and the gradient program was as follows: 90:10 V/V at 0 min, 90:10 V/V at 10 min, 40:60 V/V at 30 min, 40:60 V/V at 50 min, 90:10 V/V at 50.1 min, and 90:10 V/V at 60 min.

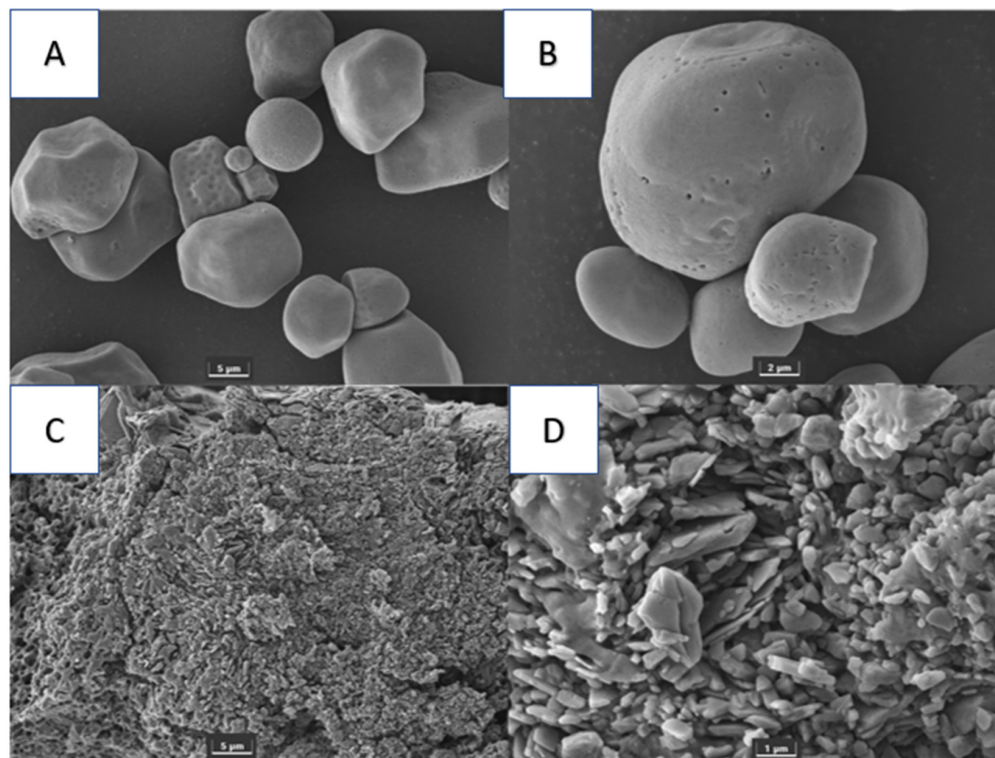


**Figure 3.** SEM photographs: initial starch (magnification 2000 (A) and 5000 (B)); causticized starch (magnification 2000 (C) and 10,000 (D)).

Data were acquired on ICS5000 (Thermo Scientific, Waltham, MA, USA), and processed using chromeleon 7.2 CDS (Thermo Scientific) [40]. Quantified data were output into excel format.

#### 2.4. Micro-Flotation Experiments

The micro-flotation tests were carried out in an XFG-1600 flotation machine with a 40 mL Plexiglass cell at a rotating speed of 1800 r/min [41]. The single mineral suspensions were prepared by adding 2.0 g of pentlandite or serpentine to 40 mL of water. The mixed mineral suspensions were prepared by adding 1.0 g of pentlandite and 1.0 g serpentine to a micro-flotation cell with 40 mL water. NaOH or HCl solutions acted as the pH regulator to adjust the pH to the desired value, and the depressant (causticized starch), collector (PBX), and frother (MIBC) were added to the suspension in sequence, with 2 min of agitation after each addition. Hereafter, the flotation was conducted for a period of 3 min. The floated and unfloated minerals were collected, filtered, and dried to calculate flotation recovery and determine the ore grade.

#### 2.5. Zeta Potential Measurements

Zeta potential measurement was carried out using a Malvern Zetasizer nano ZS zeta potential meter (Bruker Instruments Ltd., Karlsruhe, Germany). The ionic strength of the sample solution was maintained with  $1 \times 10^{-3}$  mol/L potassium nitrate ( $\text{KNO}_3$ ). The mineral suspension was prepared by adding a 30 mg sample to 10 mL of  $\text{KNO}_3$  electrolyte solution in the absence and presence of depressants for each test. The desired pH value above the solution was adjusted by adding hydrochloric acid (HCl) or sodium hydroxide (NaOH) stock solutions. The supernatant was then measured using the zeta potential

analyzer after stirring for 10 min and standing for 5 min. Each zeta potential was tested three times, and the average value was calculated and recorded.

### 2.6. FT-IR Experiments

The Fourier transform infrared spectra (FTIR) of mineral samples obtained from micro-flotation was recorded using a Nicolet iS20 (Thermo Fisher Scientific, Waltham, MA, USA). After obtaining the flotation concentrate samples in the presence or absence of depressants, the mineral samples were washed repeatedly with deionized water, then put into a vacuum oven, and dried at 35 °C for testing. The dried flotation concentrate samples were mixed with KBr in an identical proportion (1:100) to prepare the powder mixtures needed for the FT-IR spectrometer, and therefore the absorbance in their infrared spectra was proportional to the concentration of the species present in these samples.

### 2.7. XPS Analysis

X-ray photoelectron spectroscopy (XPS) measurements were performed using the Thermo Scientific K-Alpha (Thermo Scientific Co., Waltham, MA, USA) spectrometer. For each test, 1 g of serpentine was mixed with a 20 mg/L depressant solution. The solution was filtered and washed three times using milli-Q water. The filtered solids were dried in a vacuum drying oven at 35 °C and then analyzed using XPS. All binding energies were referenced to the neutral C1s peak at 284.80 eV to compensate for the surface charge effect.

## 3. Results

### 3.1. Branched Chain Length of Amylopectin

Branched chain plays a major role in the application of causticized starch, and as a result, the branched chain length of amylopectin has a decisive influence on the depression effect of causticized starch. Chromatograms analysis was used to determine the branched chain length distributions of amylopectin isolated from different causticized starches (Figure 4), and the computed results are summarized in Table 1.

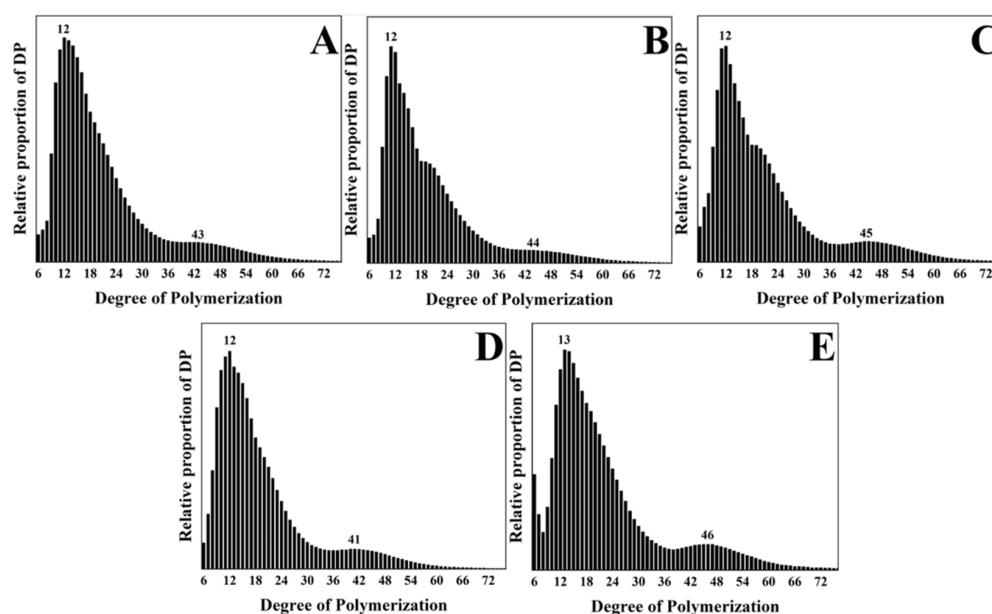


**Figure 4.** Amylopectin branched chain length distributions of different varieties of starch: (A) corn starch; (B) wheat starch (C) cassava starch; (D) rice starch; (E) potato starch.

**Table 1.** Branched chain length distributions of amylopectin.

Species	Average CL	% Distribution			
		DP 6–12	DP 13–24	DP 25–36	DP ≥ 37
Corn starch	21.21	26.69	46.62	13.71	12.98
Wheat starch	19.97	28.62	47.89	14.01	9.48
Cassava starch	22.27	19.23	51.76	14.98	14.03
Rice starch	19.48	29.62	49.12	11.15	10.11
Potato starch	20.75	23.47	51.83	13.74	10.96

In general, five kinds of causticized starches had a first peak at DP 12–13 at short chain lengths and a second peak at DP 41–46 at long chain lengths (Figure 4). Corn starch (Figure 4A) exhibited a gradual increase in chains of the polymerization degree (DP) 6–12, and formed two peaks at DP 12 and 43. Wheat starch (Figure 4B) also had a gradual increase in chains of the polymerization degree (DP) 6–12, and formed two peaks at DP 12 and 44. Moreover, it exhibited a low proportion of very long chains (DP ≥ 37) and this starch displayed a shoulder at DP 18–24. These results are in agreement with those reported by Jane et al. [8]. Cassava starch (Figure 4C) had a distribution similar to that of wheat starch, but the relative intensity of the shoulder was lower, which is in agreement with the report of Santacruz et al. [42]. A low proportion of very short chains (DP 6–12) and a high proportion of very long chains (DP ≥ 37) in branched chain length distributions were observed for the amylopectin isolated from cassava starch (Table 1). Rice starch (Figure 4D) did not show a shoulder on its distribution; in addition, it exhibited the lowest proportion of very short chains (DP 6–12) (Table 1). Potato starch (Figure 4E) displayed a trough at DP 6–10 and did not show a shoulder on its distribution. A similar distribution was found by Yoo et al. [43] in potato starch.

The distribution results of wheat starch suggested that DP 18–21 represented the full length of the crystalline region, and the ratio of the intensities of peak 1 and the shoulder indicated the proportion of short chains in the crystallites that result in defects [44], which could affect the flotation performance.

The large proportion of short chains and the small proportion of chains of DP 13–36 in rice starch may form a weak crystalline structure, which is unable to hold the clusters together or maintain the integrity of starch granules, as observed by Jane et al. in the case of sugary-2 maize starch [45]. This phenomenon may also influence the flotation performance.

In Table 1, the difference in the branched chain length distribution of the five starches is more obvious. It is not difficult to see that the average branched chain length of cassava and corn starch is the largest, followed by potato and wheat starch, with rice starch exhibiting the smallest length. At present, the starch depressants used in flotation are mostly from cassava and corn [46–51].

### 3.2. Flotation Experiments Results

Single mineral micro-flotation experiments were carried out to evaluate the depression effect of five kinds of causticized starches on serpentine and pentlandite in different flotation conditions (depressant dosage and pH value).

First, the single mineral flotation of serpentine (Figure 5A) and pentlandite (Figure 5B) was studied with different depressant dosages. The results indicated that causticized starches could effectively depress the floatation of serpentine particles, and the depression effects of five kinds of causticized starches were obviously different, especially in the depressant dosage range between 10–18 mg/L. It is worth noting that the depression effects of five causticized starches were positively correlated with the average branched chain length of these starches, i.e., the depression effects were as follows: cassava starch > corn starch > potato starch > wheat starch > rice starch. The recovery of pentlandite could maintain high values in the depressant dosage range tested (72–95%), especially in the depressant dosage range between 0–10 mg/L (>88%). In addition, the recovery of pentlandite using five causticized starches was almost indistinguishable, which was

most likely due to the difference in the interaction of causticized starch with serpentine and pentlandite. According to the results of the dosage experiments, the optimal reagent dosage of causticized starches used as a depressant was 10 mg/L for the subsequent tests.

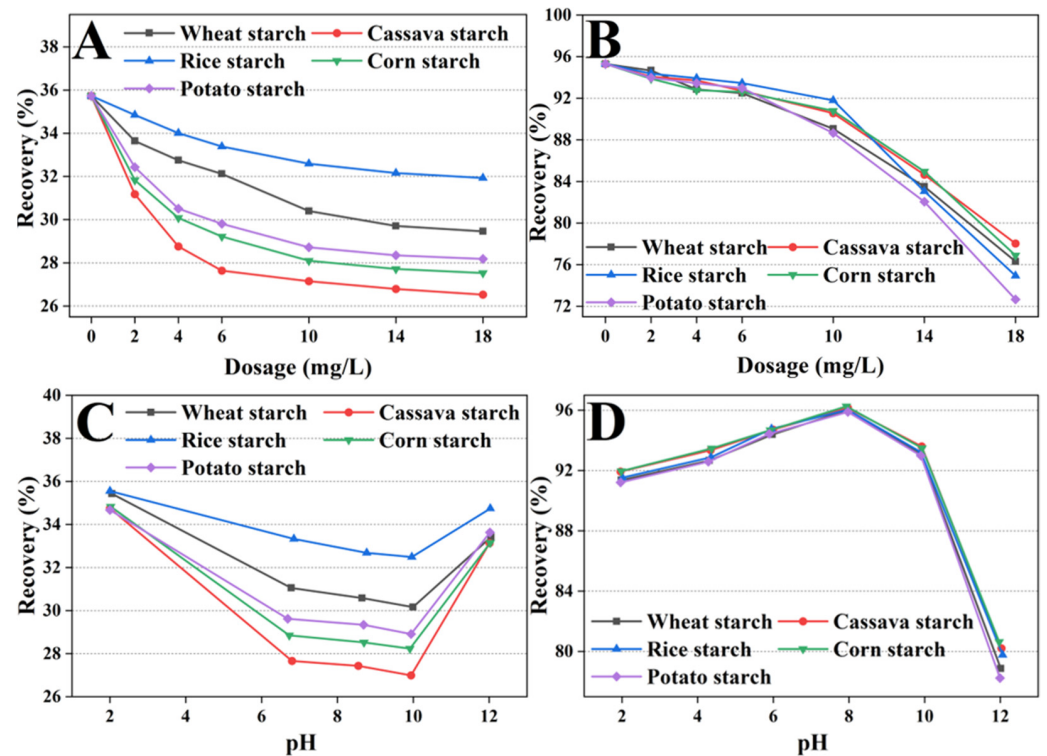


**Figure 5.** Recovery of serpentine (A,C) and pentlandite (B,D) as a function of the depressant dosage or the pH value ( $[PBX] = 1 \times 10^{-4}$  mol/L;  $[MIBC] = 1 \times 10^{-4}$  mol/L).

Next, under the optimal depressant dosage, the single mineral flotation of serpentine (Figure 5C) and pentlandite (Figure 5D) was studied at different pH values. The results of flotation tests indicated that, in the range of pH 6–10, the recovery of serpentine decreased gradually with the increase in pH value; in the range of pH 10–12, the recovery of serpentine increased with the increase in pH value. On the contrary, the recovery of pentlandite increased with increasing pH value in the pH range of 2–8, but in the range of pH 8–12, the recovery of pentlandite decreased with increasing pH value. This could be for two reasons: when the pulp pH value was more than 8, the xanthate may gradually decompose into thiocarbonates, which have no collecting ability [52], resulting in a lower collection efficiency; in the range of pH 8–12, some changes occurred on the surface of pentlandite (e.g., the formation of Ni hydroxide or Fe hydroxide [53]), resulting in reduced floatability of sulfide mineral. Dihydrocarbyl thiophosphates can be used as a sulfide collector in future research as their properties are more stable than those of butyl xanthate. As can be seen in the trend in Figure 5C,D, pH 9 was employed in follow-up flotation experiments.

After establishing the optimal flotation conditions (the dosage of depressant and the pH value of the pulp), the depression effect of different causticized starches on serpentine in the flotation of artificial mixed ore (pentlandite/serpentine system) was further investigated, and the results are shown in Figure 6 and Table 2. It was apparent that the depression effect of cassava starch and corn starch on serpentine was similar and the most effective, followed by potato starch and wheat starch, while rice starch exhibited the worst performance, i.e., close to the flotation effect without a depressant. Obviously, both single-mineral flotation experiments and mixed-mineral flotation experiments reached the same conclusion, i.e., the depression effect of causticized starches on serpentine exhibited a positive correlation with the average branched chain length. This may be due to the fact that starch with a longer branched chain could adsorb more serpentine particles.

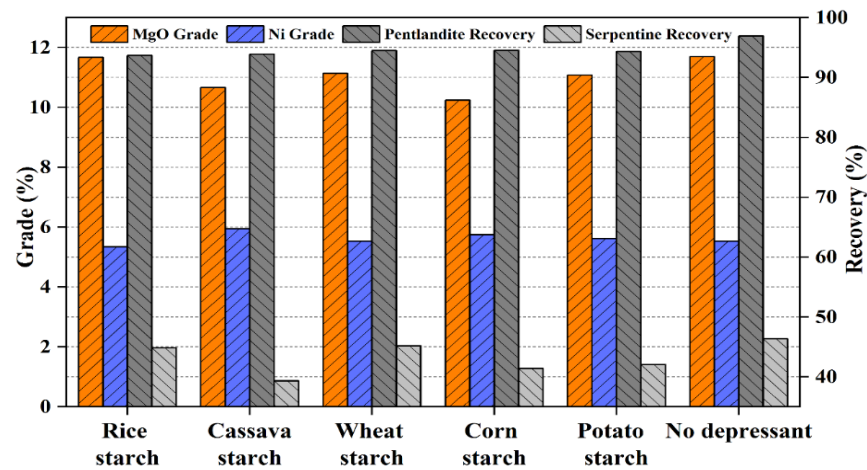


Figure 6. Recovery and grades of concentrate in the flotation of artificial mixed mineral with different causticized starches as depressants (pH = 9; [PBX] = 1 × 10<sup>-4</sup> mol/L; [MIBC] = 1 × 10<sup>-4</sup> mol/L).

Table 2. Flotation separation of mixed mineral with different causticized starch depressants.

Depressant	MgO Grade (%)	MgO Recovery (%)	Ni Grade (%)	Ni Recovery (%)
No depressant	11.69	46.35	5.53	96.92
Wheat starch	11.67	44.85	5.34	93.68
Cassava starch	10.66	39.32	5.94	93.86
Rice starch	11.13	45.18	5.53	94.47
Corn starch	10.24	41.38	5.75	94.52
Potato starch	11.08	42.03	5.62	94.34

### 3.3. Zeta Potential Measurements Results

One of the key factors that effects causticized starches’ ability to depress the flotation of serpentine is its electro-kinetic behavior [32]. Therefore, in order to further explore the reasons for and mechanism of the difference in flotation effect of causticized starches, zeta potential measurements were performed. The test results are shown in Figure 7.

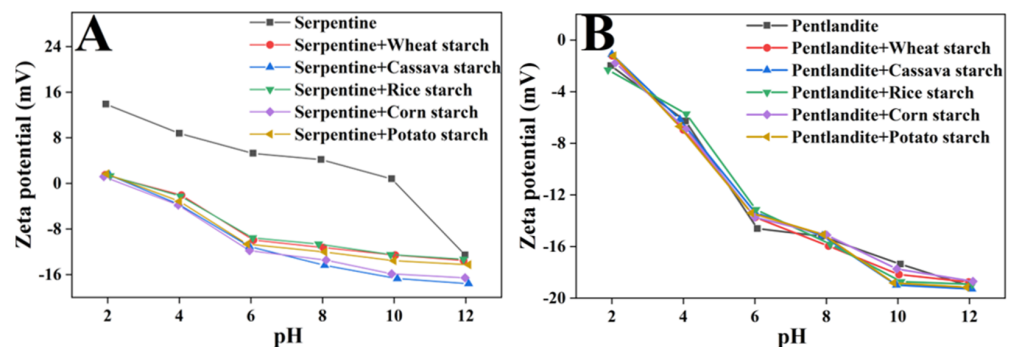


Figure 7. Zeta potentials of serpentine (A) and pentlandite (B) as a function of pH in the presence and absence of depressants (1 × 10<sup>-2</sup> g/L).

As shown in Figure 7A, the addition of causticized starches caused the zeta potential of serpentine to exhibit negative shifts. This change in zeta potential may be attributed to the interaction between the oxygenated hydrocarbon chains on the polymer (starch) and the hydroxylated metal ions on the serpentine surface, a mechanism that has also been studied before [54]. Moreover, the five kinds of causticized starches decreased the zeta potential of serpentine to different degrees. The decreasing degree was in the following order: cassava starch > corn starch > potato starch > wheat starch > rice starch. However,

the addition of causticized starches did not seem to have a significant effect on the zeta potential of pentlandite, which indicated that the adsorption of causticized starch on the surface of pentlandite was very weak.

In addition, the zeta potential measurement further elaborated the reasons for the difference in the depression effect of the five causticized starches on serpentine in the flotation of the pentlandite/serpentine system. When no depressant was added (with a natural pH value of 9), the zeta potentials of serpentine and pentlandite were positive and negative, respectively, which led to the phenomenon of electrostatic attraction between the two minerals and deteriorated their flotation separation ability [17]. When adding five kinds of causticized starches, the zeta potential of serpentine exhibited different degrees of reduction, which also reduced the effect that electrostatic attraction had on flotation to varying degrees. Therefore, the zeta potential measurement illustrated that the difference in the depression effect of five causticized starches on serpentine was caused by their different abilities to decrease serpentine's potential.

### 3.4. FT-IR Experiments Results

To further investigate the depression effect of different causticized starches on serpentine, flotation concentrates with different depressants were collected for FTIR analysis. The results are shown in Figure 8. In Figure 8, the sharp peak at  $3677\text{ cm}^{-1}$  was due to the stretching vibration of -OH, which is a characteristic and unique peak of serpentine [55]. The FTIR test results verified the adsorption of the serpentine "slime coating" on the surface of the pentlandite (serpentine is a hydrophilic mineral and therefore it should not reach the concentrate except by entrainment or if it is attached to pentlandite [17,56]). Due to the test sample preparation, the absorbance in their infrared spectra was proportional to the concentration of the species present in these test samples. Therefore, the FTIR test results could further prove that the depression effect of different causticized starches on serpentine was different, which was consistent with the results of the flotation experiment and zeta potential measurements. In conjunction with Section 3.1, it can be seen that causticized starches with longer branched chains could better disperse the serpentine particles from pentlandite and thus allow reduce the amount of serpentine adhering to the pentlandite.

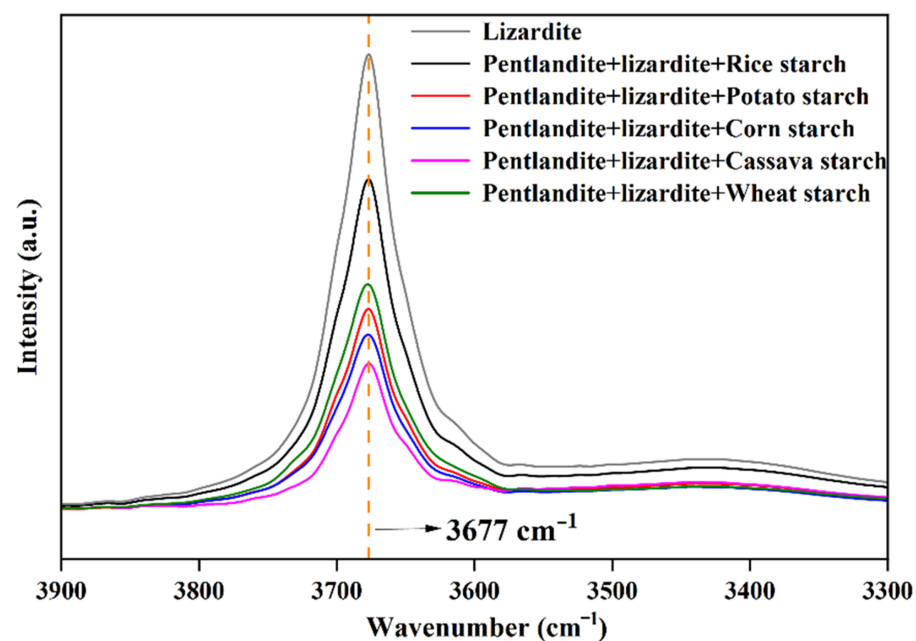


**Figure 8.** Infrared spectra of serpentine and flotation concentrate mineral samples of pentlandite mixed with serpentine in the absence and presence of  $2 \times 10^{-2}$  g/L of depressants (pH = 9; [pentlandite] = 25 g/L; [serpentine] = 25 g/L).

### 3.5. XPS Analysis Results

Even though some indication of the interaction between depressant molecules and mineral surfaces were provided in the IR spectroscopy, some significant chemical bonds on the mineral surface and the imperceptible changes of certain atoms on the mineral surface could not be characterized in this manner. XPS analysis can be used precisely determine the chemical state and elemental composition of a mineral surface and is utilized to study the interaction between depressants and serpentine [54,57–59]. Therefore, in order to further explore the interaction of the five causticized starches on the serpentine surface and what changes occurred to the serpentine surface, XPS analysis was performed. The results are shown in Figure 9 and Table 3.

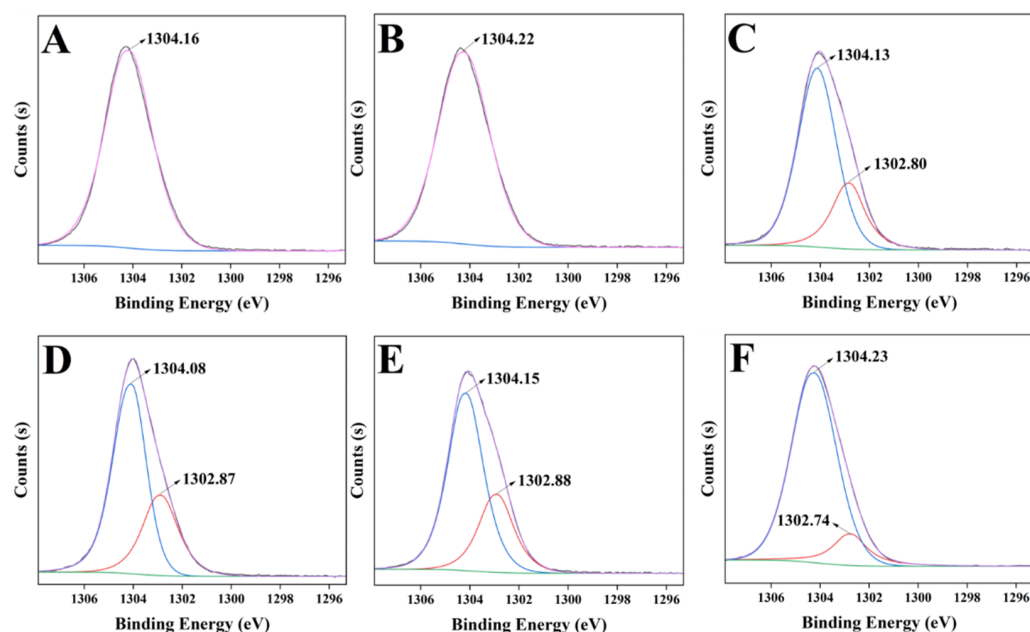


**Figure 9.** Mg 1s XPS spectra of clean serpentine surface (A) and the serpentine surfaces interacted with rice starch (B), potato starch (C), cassava starch (D), corn starch (E), and wheat starch (F).

**Table 3.** Quantification of Mg 1s species in serpentine and depressant-treated serpentine samples.

Sample	Mg 1s Binding Energy (eV)	Species Distribution (%)
Serpentine	—	0.00
	1304.16	100.00
Serpentine + Rice starch	—	0.00
	1304.22	100.00
Serpentine + Potato starch	1302.80	25.71
	1304.13	74.29
Serpentine + Cassava starch	1302.87	31.76
	1304.08	68.24
Serpentine + Corn starch	1302.88	30.26
	1304.15	69.74
Serpentine + Wheat starch	1302.74	13.33
	1304.23	86.67

In the Mg 1s spectrum shown in Figure 9A, the Mg 1s peak of bare serpentine appears at approximately 1304.16 eV in Mg-OH, as in previous studies [58,59]. In Figure 9B, it can be seen that no new peaks appeared on the surface of the serpentine treated with rice starch, which indicated that there was almost no chemical adsorption between rice starch and the serpentine surface. Figure 9C–F showed the Mg 1s spectrum obtained after adding other causticized starches, where the new Mg 1s peaks at 1302.80 eV, 1302.87 eV, 1302.88 eV

and 1302.74 eV are assigned to Mg-OR (R refers to hydrocarbon chain) on the serpentine surface [60,61], evidencing chemisorption between the causticized starches and the Mg sites of the serpentine surface. It can be seen that the interaction between the causticized starch and serpentine was mainly through the oxygen atoms of the branched chains combining with the Mg atoms on the serpentine surface.

Moreover, the element atomic content analysis in Table 3 showed the proportion of Mg atoms in different states. The results in Table 3 proved that the proportion of Mg atoms adsorbed by the five kinds of causticized starches was different, and the proportions were arranged in the following order: cassava starch > corn starch > potato starch > wheat starch > rice starch.

By combining the results of the branched chain length distribution with those of the XPS analysis, it can be concluded that the causticized starches with longer branched chains were adsorbed more strongly on serpentine surface, and thus had a better depression effect. Based on this idea, Figure 10 shows the influence mechanism of the branched chain length on the depression effect on serpentine. It can be seen from Figure 10 that the branched chain length is a crucial factor in the depression effect of causticized starch on serpentine in the flotation of the pentlandite/serpentine system.

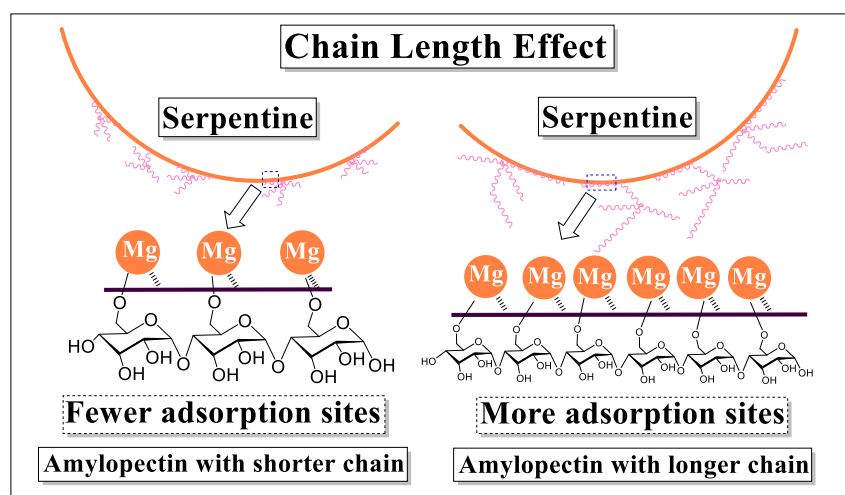


**Figure 10.** The schematic diagram for the interactions between depressants and serpentine.

#### 4. Conclusions

In this study, a method of examining the influence of different types of starches is presented through flotation experiments and mechanism studies. The following significant conclusions were drawn:

1. The results of the flotation experiments fully illustrated that the depression effect of causticized starches on serpentine were ranked as follows: cassava starch > corn starch > potato starch > wheat starch > rice starch.
2. The average branched chain length was arranged in the following order: cassava starch > corn starch > potato starch > wheat starch > rice starch, and the depression effect of causticized starches on serpentine exhibited a positive correlation with the average branched chain length.
3. Starch depressants depress the serpentine in the flotation system by combining the oxygen atoms on the oxygen-containing hydrocarbon chain with the Mg atoms on serpentine surface. Moreover, causticized starches with longer branched chains were adsorbed more strongly on serpentine surface, and thus had a better depression effect.

**Author Contributions:** Conceptualization, C.Z., F.Y. and Y.T.; methodology, C.Z. and F.Y.; formal analysis, C.Z. and J.W.; investigation, C.Z. and F.Y.; data curation, C.Z., F.Y. and Y.T.; writing—original draft preparation, C.Z.; writing—review and editing, J.C. and L.W.; supervision, J.C. and L.W.; funding acquisition, J.C. All authors have read and agreed to the published version of the manuscript.

**Funding:** This research was funded by the National Natural Science Foundation of China (52004336), State Key Laboratory of Comprehensive Utilization of Nickel and Cobalt Resources (GZSYS-KY-2020-014), Open Foundation of State Key Laboratory of Mineral Processing (BGRIMM-KJSKL-2021-06), Science and technology innovation leading project of high-tech industry of Hunan Province, China (2020GK2067), Open Fund of Key Laboratory of Metallogenic Prediction of Nonferrous Metals and Geological Environment Monitoring (Central South University) and Ministry of Education, China (2022YSJS15), National Key R&D Program of China (2019YFC1803503) and Graduate Research Innovation Project of Central South University (2022ZZTS0564).

**Data Availability Statement:** Data are available from the authors upon reasonable request.

**Conflicts of Interest:** The authors declare no conflict of interest.

## References

1. Ojogbo, E.; Ogunsona, E.O.; Mekonnen, T.H. Chemical and physical modifications of starch for renewable polymeric materials. *Mater. Today Sustain.* **2020**, *7–8*, 25. [\[CrossRef\]](#)
2. Le Corre, D.; Bras, J.; Dufresne, A. Starch Nanoparticles: A Review. *Biomacromolecules* **2010**, *11*, 1139–1153. [\[CrossRef\]](#) [\[PubMed\]](#)
3. Singh, S.; Singh, N.; Isono, N.; Noda, T. Relationship of Granule Size Distribution and Amylopectin Structure with Pasting, Thermal, and Retrogradation Properties in Wheat Starch. *J. Agric. Food Chem.* **2010**, *58*, 1180–1188. [\[CrossRef\]](#) [\[PubMed\]](#)
4. Jane, J.-I.; Atichokudomchai, N.; Park, J.-H.; Suh, D.-S. Effects of Amylopectin Structure on the Organization and Properties of Starch Granules. In *Advances in Biopolymers*; ACS Symposium Series: Washington, DC, USA, 2006; pp. 146–164.
5. Buleon, A.; Colonna, P.; Planchot, V.; Ball, S. Starch granules: Structure and biosynthesis. *Int. J. Biol. Macromol.* **1998**, *23*, 85–112. [\[CrossRef\]](#)
6. Copeland, L.; Blazek, J.; Salman, H.; Tang, M.C. Form and functionality of starch. *Food Hydrocoll.* **2009**, *23*, 1527–1534. [\[CrossRef\]](#)
7. Lin, L.; Guo, K.; Zhang, L.; Zhang, C.; Liu, Q.; Wei, C. Effects of molecular compositions on crystalline structure and functional properties of rice starches with different amylopectin extra-long chains. *Food Hydrocoll.* **2019**, *88*, 137–145. [\[CrossRef\]](#)
8. Jane, J.; Chen, Y.Y.; Lee, L.F.; McPherson, A.E.; Wong, K.S.; Radosavljevic, M.; Kasemsuwan, T. Effects of amylopectin branch chain length and amylose content on the gelatinization and pasting properties of starch. *Cereal Chem.* **1999**, *76*, 629–637. [\[CrossRef\]](#)
9. Menzel, C.; Andersson, M.; Andersson, R.; Vazquez-Gutierrez, J.L.; Daniel, G.; Langton, M.; Gallstedt, M.; Koch, K. Improved material properties of solution-cast starch films: Effect of varying amylopectin structure and amylose content of starch from genetically modified potatoes. *Carbohydr. Polym.* **2015**, *130*, 388–397. [\[CrossRef\]](#)
10. Wang, H.; Feng, L.; Manica, R.; Liu, Q. Selective depression of millerite ( $\beta$ -NiS) by polysaccharides in alkaline solutions in Cu-Ni sulphides flotation separation. *Miner. Eng.* **2021**, *172*, 107139. [\[CrossRef\]](#)
11. Qin, W.; Wei, Q.; Jiao, F.; Yang, C.; Liu, R.; Wang, P.; Ke, L. Utilization of polysaccharides as depressants for the flotation separation of copper/lead concentrate. *Int. J. Min. Sci. Technol.* **2013**, *23*, 179–186. [\[CrossRef\]](#)
12. Khoso, S.A.; Gao, Z.; Tian, M.; Hu, Y.; Sun, W. Adsorption and depression mechanism of an environmentally friendly reagent in differential flotation of Cu-Fe sulphides. *J. Mater. Res. Technol.* **2019**, *8*, 5422–5431. [\[CrossRef\]](#)
13. Sarquis, P.E.; Menéndez-Aguado, J.M.; Mahamud, M.M.; Dzioba, R. Tannins: The organic depressants alternative in selective flotation of sulfides. *J. Clean. Prod.* **2014**, *84*, 723–726. [\[CrossRef\]](#)
14. Li, M.; Liu, J.; Hu, Y.; Gao, X.; Yuan, Q.; Zhao, F. Investigation of the specularite/chlorite separation using chitosan as a novel depressant by direct flotation. *Carbohydr. Polym.* **2020**, *240*, 116334. [\[CrossRef\]](#) [\[PubMed\]](#)
15. Zhang, H.; Xu, Z.; Sun, W.; Chen, D.; Li, S.; Han, M.; Yu, H.; Zhang, C. Selective adsorption mechanism of dodecylamine on the hydrated surface of hematite and quartz. *Sep. Purif. Technol.* **2021**, *275*, 119137. [\[CrossRef\]](#)
16. Zhang, X.; Han, Y.; Gao, P.; Gu, X.; Wang, S. Depression Mechanism of a Novel Depressant on Serpentine Surfaces and Its Application to the Selective Separation of Chalcopyrite from Serpentine. *Miner. Process. Extr. Metall. Rev.* **2020**, *43*, 373–379. [\[CrossRef\]](#)
17. Bremmell, K.E.; Fornasiero, D.; Ralston, J. Pentlandite–lizardite interactions and implications for their separation by flotation. *Colloids Surf. A Physicochem. Eng. Asp.* **2005**, *252*, 207–212. [\[CrossRef\]](#)
18. Zhang, C.; Liu, C.; Feng, Q.; Chen, Y. Utilization of N-carboxymethyl chitosan as selective depressants for serpentine on the flotation of pyrite. *Int. J. Miner. Process.* **2017**, *163*, 45–47. [\[CrossRef\]](#)
19. Cao, J.; Luo, Y.-C.; Xu, G.-Q.; Qi, L.; Hu, X.-Q.; Xu, P.-F.; Zhang, L.-Y.; Cheng, S.-Y. Utilization of starch graft copolymers as selective depressants for lizardite in the flotation of pentlandite. *Appl. Surf. Sci.* **2015**, *337*, 58–64. [\[CrossRef\]](#)
20. Long, T.; Zhao, H.; Wang, Y.; Yang, W.; Deng, S.; Xiao, W.; Lan, X.; Wang, Q. Synergistic mechanism of acidified water glass and carboxymethyl cellulose in flotation of nickel sulfide ore. *Miner. Eng.* **2022**, *181*, 107547. [\[CrossRef\]](#)

21. Beattie, D.A.; Huynh, L.; Kaggwa, G.B.; Ralston, J. Influence of adsorbed polysaccharides and polyacrylamides on talc flotation. *Int. J. Miner. Process.* **2006**, *78*, 238–249. [[CrossRef](#)]
22. Sheng, Q.; Yin, W.; Ma, Y.; Liu, Y.; Wang, L.; Yang, B.; Sun, H.; Yao, J. Selective depression of talc in azurite sulfidization flotation by tamarind polysaccharide gum: Flotation response and adsorption mechanism. *Miner. Eng.* **2022**, *178*, 107393. [[CrossRef](#)]
23. Zhao, K.; Gu, G.; Wang, C.; Rao, X.; Wang, X.; Xiong, X. The effect of a new polysaccharide on the depression of talc and the flotation of a nickel–copper sulfide ore. *Miner. Eng.* **2015**, *77*, 99–106. [[CrossRef](#)]
24. Shortridge, P.G.; Harris, P.J.; Bradshaw, D.J.; Koopal, L.K. The effect of chemical composition and molecular weight of polysaccharide depressants on the flotation of talc. *Int. J. Miner. Process.* **2000**, *59*, 215–224. [[CrossRef](#)]
25. Beattie, D.A.; Huynh, L.; Kaggwa, G.B.N.; Ralston, J. The effect of polysaccharides and polyacrylamides on the depression of talc and the flotation of sulphide minerals. *Miner. Eng.* **2006**, *19*, 598–608. [[CrossRef](#)]
26. Tian, F.; Li, P.; Cao, Y.; Hao, H.; Peng, W.; Fan, G. Selective depression of low-molecular-weight carboxylated starch in flotation separation of forsterite and ilmenite. *Colloids Surf. A Physicochem. Eng. Asp.* **2022**, *648*, 129080. [[CrossRef](#)]
27. Beaussart, A.; Parkinson, L.; Mierczynska-Vasilev, A.; Beattie, D.A. Adsorption of modified dextrans on molybdenite: AFM imaging, contact angle, and flotation studies. *J. Colloid Interface Sci.* **2012**, *368*, 608–615. [[CrossRef](#)] [[PubMed](#)]
28. Chimonyo, W.; Fletcher, B.; Peng, Y. The differential depression of an oxidized starch on the flotation of chalcopyrite and graphite. *Miner. Eng.* **2020**, *146*, 106114. [[CrossRef](#)]
29. Li, H.P.; Zhang, S.S.; Jiang, H.; Li, B. Effect of modified starches on depression of diaspore. *Trans. Nonferrous Met. Soc. China* **2010**, *20*, 1494–1499. [[CrossRef](#)]
30. Feng, B.; Peng, J.; Zhang, W.; Luo, G.; Wang, H. Removal behavior of slime from pentlandite surfaces and its effect on flotation. *Miner. Eng.* **2018**, *125*, 150–154. [[CrossRef](#)]
31. Alvarez-Silva, M.; Uribe-Salas, A.; Waters, K.E.; Finch, J.A. Zeta potential study of pentlandite in the presence of serpentine and dissolved mineral species. *Miner. Eng.* **2016**, *85*, 66–71. [[CrossRef](#)]
32. Cao, J.; Hu, X.-Q.; Luo, Y.-C.; Qi, L.; Xu, G.-Q.; Xu, P.-F. The role of some special ions in the flotation separation of pentlandite from lizardite. *Colloids Surf. A Physicochem. Eng. Asp.* **2016**, *490*, 173–181. [[CrossRef](#)]
33. Huang, J.W.; Zhang, C.Q. Inhibiting effect of citric acid on the floatability of serpentine activated by Cu(II) and Ni(II) ions. *Physicochem. Probl. Miner. Process.* **2019**, *55*, 960–968. [[CrossRef](#)]
34. Ai, G.; Huang, K.; Liu, C.; Yang, S. Exploration of amino trimethylene phosphonic acid to eliminate the adverse effect of seawater in molybdenite flotation. *Int. J. Min. Sci. Technol.* **2021**, *31*, 1129–1134. [[CrossRef](#)]
35. Panda, L.; Venugopal, R.; Mandre, N.R. Selective Flocculation of Chromite Tailings. *Trans. Indian Inst. Met.* **2021**, *74*, 619–628. [[CrossRef](#)]
36. Rohem Peçanha, E.; da Fonseca de Albuquerque, M.D.; Antoun Simão, R.; de Salles Leal Filho, L.; de Mello Monte, M.B. Interaction forces between colloidal starch and quartz and hematite particles in mineral flotation. *Colloids Surf. A Physicochem. Eng. Asp.* **2019**, *562*, 79–85. [[CrossRef](#)]
37. Ren, Z.T.; He, S.Z.; Zhao, N.; Zhai, H.; Liu, Q.C. A sucrose non-fermenting-1-related protein kinase-1 gene, IbSnRK1, improves starch content, composition, granule size, degree of crystallinity and gelatinization in transgenic sweet potato. *Plant Biotechnol. J.* **2019**, *17*, 21–32. [[CrossRef](#)]
38. Nishi, A.; Nakamura, Y.; Tanaka, N.; Satoh, H. Biochemical and genetic analysis of the effects of amylose-extender mutation in rice endosperm. *Plant Physiol.* **2001**, *127*, 459–472. [[CrossRef](#)]
39. Liu, W.-C.; Halley, P.J.; Gilbert, R.G. Mechanism of Degradation of Starch, a Highly Branched Polymer, during Extrusion. *Macromolecules* **2010**, *43*, 2855–2864. [[CrossRef](#)]
40. Zhou, W.Z.; Yang, J.; Hong, Y.; Liu, G.L.; Zheng, J.L.; Gu, Z.B.; Zhang, P. Impact of amylose content on starch physicochemical properties in transgenic sweet potato. *Carbohydr. Polym.* **2015**, *122*, 417–427. [[CrossRef](#)]
41. Tang, X.; Chen, Y. Using oxalic acid to eliminate the slime coatings of serpentine in pyrite flotation. *Miner. Eng.* **2020**, *149*, 106228. [[CrossRef](#)]
42. Santacruz, S.; Koch, K.; Svensson, E.; Ruales, J.; Eliasson, A.C. Three underutilised sources of starch from the Andean region in Ecuador Part 1. Physico-chemical characterisation. *Carbohydr. Polym.* **2002**, *49*, 63–70. [[CrossRef](#)]
43. Yoo, S.H.; Perera, C.; Shen, J.F.; Ye, L.Y.; Suh, D.S.; Jane, J.L. Molecular Structure of Selected Tuber and Root Starches and Effect of Amylopectin Structure on Their Physical Properties. *J. Agric. Food Chem.* **2009**, *57*, 1556–1564. [[CrossRef](#)] [[PubMed](#)]
44. Genkina, N.K.; Wikman, J.; Bertoft, E.; Yuryev, V.P. Effects of structural imperfection on gelatinization characteristics of amylopectin starches with A- and B-type crystallinity. *Biomacromolecules* **2007**, *8*, 2329–2335. [[CrossRef](#)] [[PubMed](#)]
45. Jane, J.; Atichokudomchai, N.; Suh, D.S. Internal structures of starch granules revealed by confocal laser-light scanning microscopy. In *Starch: Progress in Structural Studies, Modifications and Applications*; Polish Society of Food Technologists: Malopolsks, Poland, 2004; pp. 147–156.
46. Marins, T.F.; Rodrigues, O.M.S.; Reis, E.L.; Beltrao, J.G. Utilising starches from sugarcane and cassava residues as hematite depressants. *Miner. Eng.* **2020**, *145*, 5. [[CrossRef](#)]
47. Li, W.B.; Shi, D.; Han, Y.X. A selective flotation of fluorite from dolomite using caustic cassava starch and its adsorption mechanism: An experimental and DFT Study. *Colloid Surf. A-Physicochem. Eng. Asp.* **2022**, *633*, 9. [[CrossRef](#)]
48. Yang, S.Y.; Li, C.; Wang, L.G. Dissolution of starch and its role in the flotation separation of quartz from hematite. *Powder Technol.* **2017**, *320*, 346–357. [[CrossRef](#)]

49. Shrimali, K.; Atluri, V.; Wang, Y.; Bacchuwar, S.; Wang, X.M.; Miller, J.D. The nature of hematite depression with corn starch in the reverse flotation of iron ore. *J. Colloid Interface Sci.* **2018**, *524*, 337–349. [[CrossRef](#)]
50. Peng, W.J.; Zhang, L.Y.; Qiu, Y.S.; Song, S.X. Depression effect of corn starch on muscovite mica at different pH values. *Physicochem. Probl. Miner. Process.* **2016**, *52*, 780–788. [[CrossRef](#)]
51. Deng, J.; Yang, S.Y.; Liu, C.; Li, H.Q. Effects of the calcite on quartz flotation using the reagent scheme of starch/dodecylamine. *Colloid Surf. A-Physicochem. Eng. Asp.* **2019**, *583*, 6. [[CrossRef](#)]
52. Batanero, B.; Picazo, O.; Barba, F. Facile and efficient transformation of xanthates into thiocarbonates by anodic oxidation. *J. Org. Chem.* **2001**, *66*, 320–322. [[CrossRef](#)]
53. Legrand, D.L.; Bancroft, G.M.; Nesbitt, H.W. Oxidation/alteration of pentlandite and pyrrhotite surfaces at pH 9.3: Part 1. Assignment of XPS spectra and chemical trends. *Am. Miner.* **2005**, *90*, 1042–1054. [[CrossRef](#)]
54. Liu, C.; Zheng, Y.; Yang, S.; Fu, W.; Chen, X. Exploration of a novel depressant polyepoxysuccinic acid for the flotation separation of pentlandite from lizardite slimes. *Appl. Clay Sci.* **2021**, *202*, 105939. [[CrossRef](#)]
55. Wilson, M.J. Electron paramagnetic resonance spectroscopy. In *Clay Mineralogy: Spectroscopic and Chemical Determinative Methods*; Springer: Dordrecht, The Netherlands, 1994; pp. 173–225.
56. Wellham, E.J.; Elber, L.; Yan, D.S. The role of carboxy methyl cellulose in the flotation of a nickel sulphide transition ore. *Miner. Eng.* **1992**, *5*, 381–395. [[CrossRef](#)]
57. Liu, D.; Zhang, G.; Huang, G.; Gao, Y.; Wang, M. The flotation separation of pyrite from serpentine using lemon yellow as selective depressant. *Colloids Surf. A Physicochem. Eng. Asp.* **2019**, *581*, 123823. [[CrossRef](#)]
58. Liu, C.; Ai, G.; Song, S. The effect of amino trimethylene phosphonic acid on the flotation separation of pentlandite from lizardite. *Powder Technol.* **2018**, *336*, 527–532. [[CrossRef](#)]
59. Li, Z.-H.; Han, Y.-X.; Li, Y.-J.; Gao, P. Effect of serpentine and sodium hexametaphosphate on ascharite flotation. *Trans. Nonferrous Met. Soc. China* **2017**, *27*, 1841–1848. [[CrossRef](#)]
60. Milcius, D.; Grbovic-Novakovic, J.; Zostautiene, R.; Lelis, M.; Girdzevicius, D.; Urbonavicius, M. Combined XRD and XPS analysis of ex-situ and in-situ plasma hydrogenated magnetron sputtered Mg films. *J. Alloys Compd.* **2015**, *647*, 790–796. [[CrossRef](#)]
61. Jensen, I.J.T.; Thogersen, A.; Lovvik, O.M.; Schreuders, H.; Dam, B.; Diplas, S. X-ray photoelectron spectroscopy investigation of magnetron sputtered Mg-Ti-H thin films. *Int. J. Hydrogen Energy* **2013**, *38*, 10704–10715. [[CrossRef](#)]